Inorganica Chimica Acta 369 (2011) 247–252

Contents lists available at ScienceDirect

Inorganica Chimica Acta

journal homepage: www.elsevier.com/locate/ica

Cyclopalladation of *N*-phenylbenzamides: Synthesis and structure of bimetallic palladium(II)-complexes

Nadine Borduas, Alan J. Lough, Vy M. Dong *

Department of Chemistry, University of Toronto, 80 St. George Street, Toronto, Ontario, Canada M5S 3H6

ARTICLE INFO

Article history:
Available online 2 March 2011

Dedicated to Prof. Robert G. Bergman.

Keywords:
Palladium(II) dimer
C–H activation
Oxidative cross-coupling
Intramolecular reaction

ABSTRACT

Three bimetallic palladium(II) complexes were generated by cyclopalladation of *N*-methyl-*N*-phenylbenzamide derivatives, substrates known to undergo oxidative intramolecular cross-coupling via palladium catalysis. These isolable Pd-complexes were characterized by X-ray crystallography. Stoichiometric and catalytic experiments with [(3-methoxy-*N*-methyl-*N*-phenylbenzamide)Pd(μ-TFA)]$_2$ were investigated, and this palladium complex was found to be an effective precatalyst for oxidative cross-coupling.

1. Introduction

Intramolecular oxidative cross-coupling has emerged as an attractive strategy for generating cyclic architectures from relatively simple precursors [1]. This transition metal-catalyzed ring-closure involves C–C bond formation by the oxidation of two C–H bonds [2]. Our group reported the palladium-catalyzed lactam synthesis by oxidative cyclization of *N*-phenylbenzamides using sodium persulfate ($Na_2S_2O_8$) as a convenient oxidant (Fig. 1) [3]. To further study this process, we sought to isolate a Pd(II)-complex from the analogous stoichiometric reaction. We imagined that *N*-methyl-*N*-phenylbenzamide (**1a**) could undergo initial *ortho* C–H bond activation by cyclopalladation to generate either Pd(II) six-membered palladacycle **2a** or Pd(II) five-membered palladacycle **3a** (Fig. 2).

We report herein the isolation and characterization of dimeric palladium-complexes [(3-methoxy-*N*-methyl-*N*-phenylbenzamide)Pd(μ-TFA)]$_2$ (**3a**), [(3-methoxy-*N*-methyl-*N*-(*o*-tolyl)benzamide)Pd(μ-TFA)]$_2$ (**3b**) and [(3,4-dimethoxy-*N*-methyl-*N*-phenylbenzamide)Pd(μ-TFA)]$_2$ (**3c**) derived from cyclopalladation of the corresponding *N*-methyl-*N*-phenylbenzamide. The molecular structures of complexes **3a**, **3b** and **3c** were established by single-crystal X-ray structure analysis. These palladacycles were tested to their feasibility as intermediates in catalytic oxidative cross-coupling reactions.

2. Experimental

2.1. Methods and materials

^{1}H, ^{13}C{^{1}H}, and ^{19}F NMR spectra were recorded on a Varian Mercury 400 or a Bruker AV-III 400 spectrometer at ambient temperature. All NMR spectra are referenced to TMS or the residual solvent signal. Data for NMR are reported as follows: chemical shift (δ ppm), multiplicity (s = singlet, d = doublet, t = triplet, q = quartet, m = multiplet, br = broad), integration, coupling constant (Hz). High resolution mass spectra (HRMS) were recorded on a micromass 70S-250 spectrometer (EI) or an ABI/Sciex Qstar Mass Spectrometer (ESI). Column chromatography was carried out on Silicycle Silica-P Flash Silica Gel (40–63 μm). Preparative thin layer chromatography was performed on EMD Silica Gel 60 F_{254} plates (254 μm). Chemical reagents were purchased from Aldrich and Pd(OAc)$_2$ was purchased from Strem. Solvents were purchased from Sigma Aldrich and Caledon and used without further purification.

2.2. X-ray data collection and crystal structure determination

Data were collected on a Bruker-Nonius Kappa-CCD diffractometer using monochromated Mo Kα radiation and were measured using a combination of ϕ scans and ω scans with κ offsets, to fill the Ewald sphere. The data were processed using the Denzo-SMN package [4]. Absorption corrections were carried out using SORTAV [5]. The structure was solved and refined using SHELXTL V6.1 [6] for full-matrix least-squares refinement that was based on F^2. All H atoms were included in calculated positions and allowed to refine in riding-motion approximation with U_{iso} tied to the carrier atom.

* Corresponding author. Tel.: +1 416 978 6484.
E-mail address: vdong@chem.utoronto.ca (V.M. Dong).

0020-1693/$ - see front matter © 2011 Elsevier B.V. All rights reserved.
doi:10.1016/j.ica.2011.01.059

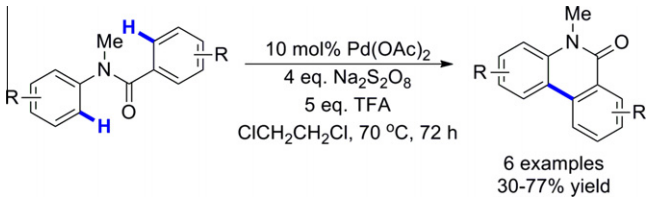

Fig. 1. Reported Pd(II)-catalyzed intramolecular oxidative cross-coupling.

2.3. Synthesis of palladium complexes

General procedure A: Palladium complexes **3a**–**3c** were prepared based on a modified literature procedure [3]. To a one-dram vial was added 3-methoxy-*N*-methyl-*N*-phenylbenzamide (**1a**) (48 mg, 0.20 mmol), $Pd(OAc)_2$ (45 mg, 0.20 mmol) and 1,2-dichloroethane (1 mL). The reaction mixture was stirred for 2 min and trifluoroacetic acid (16 μL, 0.21 mmol) was subsequently added. The resulting solution was stirred on a heating block at 40 °C for 2.5 h under air. After cooling to ambient temperature, the reaction mixture was left to stand for several minutes until a yellow precipitate was observed. The mixture was filtered through a cotton-plugged pipette and the resulting yellow residue was washed (4 × 1 mL) with dichloromethane. The filtrate was then discarded. The yellow residue was suspended in dichloromethane and subsequently transferred into a tared vial and concentrated *in vacuo* to afford the bimetallic palladacycle **3a** as a yellow solid (53 mg, 58%).

2.3.1. [(3-Methoxy-N-methyl-N-phenylbenzamide)Pd(μ-TFA)]$_2$ (**3a**)

^{1}H NMR (400 MHz, DMF-d_7) δ 7.68–7.60 (m, 5H), 6.73 (d, 1H, J = 7.3 Hz), 6.62 (d, 1H, J = 8.1 Hz), 5.31 (d, 1H, J = 1.9 Hz), 3.51 (s, 3H), 3.24 (s, 3H). ^{13}C{^{1}H} NMR (100 MHz, DMF-d_7) δ 178.4, 156.2, 143.0, 139.1, 135.8, 132.2, 131.1, 130.0, 127.9, 118.2, 114.2, 54.7, 41.0. ^{19}F NMR (376 MHz, DMF-d_7) δ −74.78.

2.3.2. [(3-Methoxy-N-methyl-N-(o-tolyl)benzamide)Pd(μ-TFA)]$_2$ (**3b**)

Prepared according to general procedure A, using 3-methoxy-*N*-methyl-*N*-(*o*-tolyl)benzamide (51 mg, 0.20 mmol) to afford the bimetallic palladacycle **3b** as a yellow solid (62 mg, 65%). ^{1}H NMR (400 MHz, DMF-d_7) δ 7.55–7.48 (m, 4H), 6.75 (dd, 1H, J = 2.2 Hz, J = 8.4 Hz), 6.64 (d, 1H, J = 7.8 Hz), 5.29 (d, 1H, J = 2.8 Hz), 3.46 (s, 3H), 3.23 (s, 3H), 2.23 (s, 3H). ^{13}C{^{1}H} NMR (100 MHz, DMF-d_7) δ 178.4, 156.5, 141.5, 139.1, 135.8, 135.6, 132.5, 132.2, 130.4, 128.9, 128.2, 118.5, 113.0, 54.8, 39.8, 16.8. ^{19}F NMR (376 MHz, DMF-d_7) δ −74.96.

2.3.3. [(3,4-Dimethoxy-N-methyl-N-phenylbenzamide)Pd(μ-TFA)]$_2$ (**3c**)

Prepared according to general procedure A, using 3,4-dimethoxy-*N*-methyl-*N*-phenylbenzamide (54 mg, 0.20 mmol) to afford the bimetallic palladacycle **3c** as a yellow solid (46 mg, 47%). ^{1}H NMR (400 MHz, DMF-d_7) δ 7.68–7.64 (m, 2H), 7.60–7.56 (m, 3H), 6.24 (s, 1H), 5.28 (s, 1H), 3.71 (s, 3H), 3.48 (s, 3H), 3.06 (s, 3H). ^{13}C{^{1}H} NMR (100 MHz, DMF-d_7) δ 178.2, 150.6, 145.7, 143.1, 131.1, 129.9, 128.2, 112.7, 112.6, 112.5, 55.3, 54.8, 40.5 (one C peak overlapping). ^{19}F NMR (376 MHz, DMF-d_7) δ −75.04.

2.4. Synthesis of phenylbenzamides

2.4.1. 3-Methoxy-N-methyl-N-(o-tolyl)benzamide (**1b**)

Prepared according to a literature procedure [3], **1b** was synthesized from *N*,2-dimethylaniline (0.62 mL, 5.0 mmol) and 3-methoxybenzoyl chloride (0.82 mL, 6.0 mmol) to afford a yellow oil after purification(1.27 g, 99%). ^{1}H NMR (400 MHz, $CDCl_3$) δ 7.13–7.07 (m, 3H), 7.04–7.00 (m, 2H), 6.85–6.83 (m, 2H), 6.75 (dd, 1H, J = 2.1 Hz, J = 8.2 Hz), 3.63 (s, 3H), 3.38 (s, 3H), 2.22 (s, 3H). ^{13}C{^{1}H} NMR (100 MHz, $CDCl_3$) δ 170.4, 158.7, 143.6, 137.0, 134.8, 131.3, 128.6, 128.5, 127.7, 127.0, 120.8, 116.2, 113.3, 55.1, 37.6, 17.8. MS (ESI) *m/z* 256 (M+H), 278 (M+Na); HRMS (ESI) *m/z* Calc. for $C_{16}H_{17}NO_2$ [M+H]$^+$: 256.1332. Found: 256.1320.

2.5. Catalytic reactions

General procedure B: Phenanthridinones **4a**–**4d** were prepared based on a modified literature procedure [3]. To a one-dram vial was added 3-methoxy-*N*-methyl-*N*-phenylbenzamide (**1a**) (48 mg, 0.20 mmol), [(3-methoxy-*N*-methyl-*N*-phenylbenzamide)Pd(μ-TFA)] (**3a**) (9.2 mg, 0.01 mmol) or $Pd(OAc)_2$ (4.5 mg, 0.02 mmol), $Na_2S_2O_8$ (190 mg, 0.80 mmol), and 1,2-dichloroethane (1 mL). The mixture was stirred at room temperature for 2 min and subsequently, tetradecane (52 μL, 0.20 mmol) and trifluoroacetic acid (77 μL, 1.0 mmol) were added. The vial was sealed under air with a Teflon cap and stirred on a heating block at 70 °C for the indicated amount of time. The reactions were monitored by GC–FID.

3. Crystallography

Recrystallization of **3a**–**3c** from *N*,*N*-dimethylformamide and ether by slow diffusion gave single crystals suitable for X-ray analysis. A perspective view of each complex **3a**, **3b** and **3c** with the pertinent atom-labeling scheme is shown in Figs. 3–5, respectively. Crystal data and refinement information for each structure is given in Table 1. Selected bond distances and angles are given in Table 2 for **3a**, **3b** and **3c**.

In all cases, the palladium atom is coordinated in a slightly distorted square plane (i.e. clamshell geometry) [7]. This geometry is also apparent through the difference in bond angles between the $O_{benzamide}$–Pd(1)–Pd(2) and O_{TFA}–Pd(1)–Pd(2) where an increase in 14–22° is observed for the open-end of the clamshell. Of note, the two arenes of the ligand are perpendicular to each other and the two ligands are oriented in a head to tail fashion. Furthermore, we observe that each palladacycle is a Pd(II)-bimetallic complex. The internuclear distance between the two Pd atoms in **3a**, **3b** and **3c** were determined to be 2.8945(6), 2.8859(6) and 2.8959(6) Å, respectively. In comparison to other Pd-complexes bearing bridging trifluoroacetate ligands, bimetallic Pd complex **3a** exhibits slightly shorter Pd–Pd bonds [8].

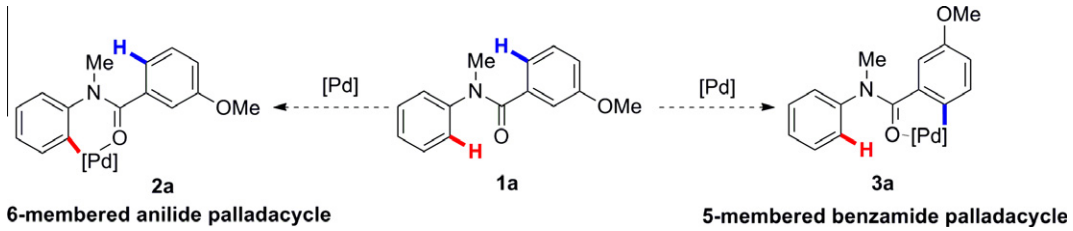

Fig. 2. Possible palladacycles from *N*-phenylbenzamide.

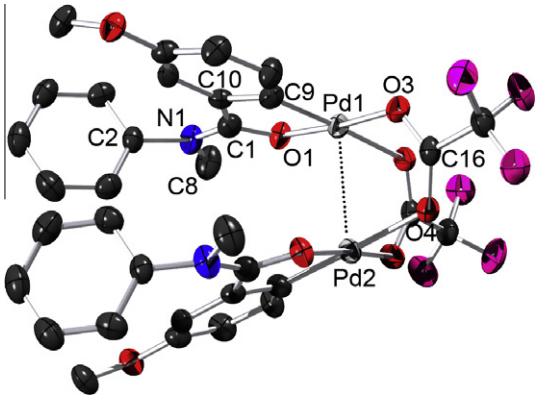

Fig. 3. ORTEP plot of [(3-methoxy-*N*-methyl-*N*-phenylbenzamide)Pd(μ-TFA)]$_2$ (**3a**). All H atoms have been omitted for clarity. Anisotropic displacement ellipsoids are shown at the 50% probability level.

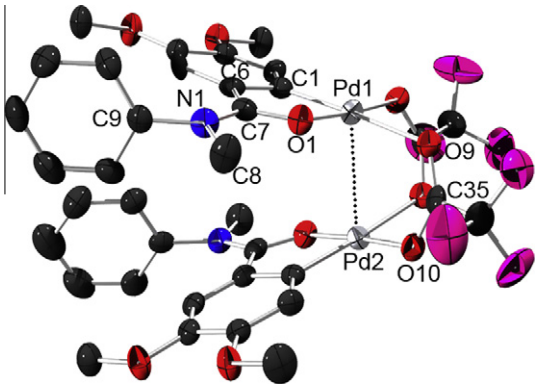

Fig. 4. ORTEP plot of [(3-methoxy-*N*-methyl-*N*-(*o*-tolyl)benzamide)Pd(μ-TFA)]$_2$ (**3b**). All H atoms have been omitted for clarity. Anisotropic displacement ellipsoids are shown at the 50% probability level.

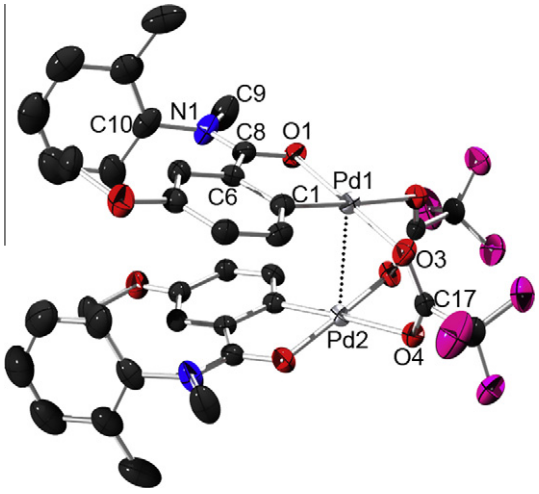

Fig. 5. ORTEP plot of [(3,4-dimethoxy-*N*-methyl-*N*-phenylbenzamide)Pd(μ-TFA)]$_2$ (**3c**). All H atoms have been omitted for clarity. Anisotropic displacement ellipsoids are shown at the 50% probability level.

4. Results and discussion

4.1. Synthesis of the palladium complexes

Pd(II)-dimers have attracted interest due to their proposed role as precursors to Pd(III)–Pd(III) or Pd(II)–Pd(IV) intermediates in C–H bond functionalizations [7,9]. For C–H bond activation of *N*-phenylbenzamides, we reasoned that either the formation of the six- or five-membered palladacycle could be possible (Fig. 2). To investigate the regioselectivity of the *ortho*-palladation, we submitted 3-methoxy-*N*-methyl-*N*-phenylbenzamide (**1a**) to stoichiometric Pd(OAc)$_2$ and trifluoroacetic acid (TFA) (Table 3, entry 1).[1] Recrystallization of the yellow solid followed by X-ray analysis of a single crystal allowed confirmation of a TFA-bridged dimeric Pd-complex (**3a**). Complexes **3b** and **3c** were obtained via an analogous method (Table 3, entries 2 and 3)[2]. In all three cases, we observed clean conversion to the thermodynamically and kinetically favored five-membered palladacycle, presumably by C–H bond activation on the benzamide ring (Fig. 6). In previous studies on intermolecular oxidative cross-couplings, six-membered palladacycles from the C–H bond activation of anilides were isolated [3]. In these studies, attempts to isolate related five-membered palladacycles derived from *N*-alkyl-benzamides had been unsuccessful.

By ^{1}H NMR analysis of **3a**, **3b**, and **3c**, the *ortho*-benzamide protons have chemical shifts ca.5.30 ppm, which is significantly more upfield than the benzamide protons of their respective starting material (chemical shifts between approximately 6.75–7.0 ppm). This observation is in agreement with the X-ray crystal structure of the complexes which show a Pd–C single bond in the solid state. ^{19}F NMR studies show that each complex possesses a single peak at a slightly different chemical shift (Table 3). We found that the Pd-complexes are unstable in solution in the presence of electrolytes.[3] The low solubility of **3a**, **3b** and **3c** in the majority of solvents prevented us from acquiring reliable photophysical data. These Pd(II)-dimers exhibit some solubility in *N*,*N*-dimethylformamide and dimethylsulfoxide. All three palladacycles are bench-stable for months provided that they are kept away from light.

4.2. Stoichiometric experiments

With the dimeric palladium complex **3a** in hand, we sought to investigate its viability as an intermediate in the catalytic cycle. Previous work in our group has demonstrated that the mechanism of oxidative cross-coupling depends on the directing group and the oxidant [2k,3]. For instance, in the *ortho*-arylation of *O*-phenylcarbamates, reductive elimination from the Pd(II) dimers was observed at 70 °C in benzene without additives, while for anilides, the isolated palladacycles underwent reductive elimination solely in the presence of TFA *and* $Na_2S_2O_8$. In the case of our intramolecular reaction, the coupling partner is part of the ligand. Therefore, for the anilide portion of the ligand to undergo C–H activation followed by reductive elimination, a rearrangement of the ligand possibly involving dissociation of the TFA or of the carbonyl of the amide, is required.

In an attempt to observe stoichiometric reductive elimination directly from **3a**, we heated a stoichiometric amount of this Pd-

[1] Pd-complex **3a** could also be obtained from the reaction of one equivalent of Pd(TFA)$_2$ and 3-methoxy-*N*-methyl-*N*-phenylbenzamide (**1a**) in 67% yield. This Pd(II)-dimer gave identical NMR data as a greenish yellow solid.

[2] Other substrates known to undergo oxidative cross-coupling under Pd(II) catalysis [3] were tested, but failed to generate an isolable Pd-complex. Further, these complexes were not observed to form in a significant amount based on NMR studies. The substitution pattern on the arene rings of the benzamide appears to impact the stability of the corresponding palladacycle.

[3] Attempts to acquire cyclic voltammetry data were unsuccessful due to the decomposition of the complexes in coordinating solvents in the presence of the electrolyte tetrabutylammonium hexafluorophosphate (TBAPF$_6$). Dissolving the complexes in acetonitrile, for example, followed by the addition of TBAPF$_6$ resulted in decomposition to Pd black. The ^{1}H NMR of this solution indicated a complex mixture of products. The complexes in acetonitrile-d3 are stable as confirmed by repeated ^{1}H NMR experiments.

Table 1
Crystal data and structure refinement for **3a**, **3b** and **3c**.

	3a	**3b**	**3c**
Empirical formula	$C_{34}H_{28}F_6N_2O_8Pd_2$	$C_{36}H_{32}F_6N_2O_{10}Pd_2$	$C_{36}H_{32}F_6N_2O_8Pd_2$
Formula weight	919.38	979.44	947.44
T (K)	150(1)	150(1)	150(1)
λ (Å)	0.71073	0.7107	0.71073
Crystal system	monoclinic	monoclinic	monoclinic
Space group	$C2/c$	$P21/n$	$C2/c$
a (Å)	20.7156(8)	12.4030(5)	19.6309(5)
b (Å)	13.0752(5)	14.8379(3)	12.8287(5)
c (Å)	15.1485(4)	20.6358(8)	17.0792(6)
α (°)	90	90	90
β (°)	124.5460(17)	97.2140(14)	124.0120(15)
γ (°)	90	90	90
V (Å^3)	3379.6(2)	3767.6(2)	3565.4(2)
Z	4	4	4
Density (calculated) (Mg/m^3)	1.807	1.727	1.765
Absorption coefficient (mm^{-1})	1.152	1.043	1.095
F(0 0 0)	1824	1952	1888
Crystal size (mm)	0.18 × 0.06 × 0.06	0.22 × 0.12 × 0.08	0.16 × 0.16 × 0.10
θ range for data collection (°)	2.74–27.50	2.75–27.55	2.86–27.53
Index ranges	$-26 \leqslant h \leqslant 26$, $-16 \leqslant k \leqslant 16$, $-16 \leqslant l \leqslant 19$	$-16 \leqslant h \leqslant 16$, $-16 \leqslant k \leqslant 19$, $-21 \leqslant l \leqslant 26$	$-25 \leqslant h \leqslant 23$, $-16 \leqslant k \leqslant 16$, $-21 \leqslant l \leqslant 22$
Reflections collected	11 009	25 472	15 737
Independent reflections (R_{int})	3847 (0.0710)	8586 (0.0777)	4067 (0.0490)
Completeness to θ = 27.50°	99.2%	98.8%	98.9%
Absorption correction		semi-empirical from equivalents	
Maximum and minimum transmission	0.937 and 0.750	0.925 and 0.831	0.901 and 0.827
Refinement method		full-matrix least-squares on F^2	
Data/restraints/parameters	3847/0/237	8586/0/511	4067/0/247
Goodness-of-fit (GOF) on F^2	1.061	1.048	1.075
Final R indices [$I > \sigma(I)$]	R_1 = 0.0471, $wR2$ = 0.1021	R_1 = 0.0604, wR_2 = 0.1246	R_1 = 0.0459, wR_2 = 0.1104
R indices (all data)	R_1 = 0.0954, wR_2 = 0.1252	R_1 = 0.1407, wR_2 = 0.1621	R_1 = 0.0754, wR_2 = 0.1281
Largest difference in peak and hole (e Å^{-3})	2.065 and −1.092	2.132 and −0.973	1.876 and −0.911

Table 2
Selected bond lengths (Å) and bond angles (°) for **3a**, **3b** and **3c**.

Bond lengths	**3a**	**3b**	**3c**
Pd(1)–Pd	2.8945(6)	2.8859(6)	2.8959(6)
Pd(1)–C	1.949(5)	1.931(6)	1.945(4)
Pd(1)–$O_{benzamide}$	2.017(3)	2.008(4)	2.024(3)
Pd(1)–$O_{TFA,\ trans\ to\ carbonyl}$	2.053(3)	2.040(4)	2.047(3)
Pd(1)–$O_{TFA,\ trans\ to\ arene}$	2.181(3)	2.179(4)	2.192(3)
$O_{carbonyl}$–$C_{carbonyl}$	1.288(5)	1.294(7)	1.272(5)
$C_{carbonyl}$–C_{arene}	1.481(6)	1.450(8)	1.487(6)
C_{arene}–C_{Pd}	1.396(6)	1.411(8)	1.408(6)
C–Pd(1)–Pd	100.80(12)	102.37(17)	102.78(12)
$O_{carbonyl}$–Pd(1)–Pd	102.55(8)	99.57(12)	98.41(9)
$O_{TFA,\ trans\ to\ carbonyl}$–Pd(1)–Pd	80.83(8)	83.35(12)	84.16(8)
$O_{TFA,\ trans\ to\ arene}$–Pd(1)–Pd	79.92(8)	78.12(11)	77.51(8)
$O_{carbonyl}$–Pd(1)–$O_{TFA,\ trans\ to\ carbonyl}$	175.16(12)	175.86(16)	175.73(11)
$O_{carbonyl}$–Pd(1)–$O_{TFA,\ trans\ to\ arene}$	92.81(12)	90.38(17)	93.34(11)
C–Pd(1)–$O_{carbonyl}$	82.06(16)	81.9(2)	81.78(15)
$O_{TFA,\ trans\ to\ carbonyl}$–$C_{TFA}$–$O_{TFA}$	130.3(4)	130.6(6)	130.5(4)
C–Pd(1)–$O_{TFA,\ trans\ to\ carbonyl}$	93.95(16)	94.6(2)	94.35(15)
$O_{TFA,\ trans\ to\ carbonyl}$–Pd(1)–$O_{TFA,\ trans\ to\ arene}$	91.18(12)	93.10(17)	90.54(12)
C_{arene}–C_{Pd}–Pd(1)	114.1(3)	114.5(4)	114.7(3)

complex in 1,2-dichloroethane at 70 °C (Fig. 7). The experiment generated no desired cross-coupled product within the time frame of the corresponding catalytic process (24 h) (Table 4, entry 1). On the other hand, if the reaction was stirred for 4 days at the same temperature, phenanthridinone **4a** could be detected by GC–FID (Table 4, entry 3). When both TFA and $Na_2S_2O_8$ were added to the reaction mixture, the reductive elimination product was detected within 24 h, but in low yield (Table 4, entry 2). Product **4a** appears to be unstable under the reaction conditions over prolonged times (Table 4, entry 4). Therefore, reductive elimination is a viable process from complex **3a** and the efficiency varies depending on the reaction conditions.

Table 3
Synthesis and characterization of the Pd-complexes.

Entry	Substrate	R^1, R^2	Pd-complex	Yield (%)	^{1}H NMR (δ) for H_{ortho} (ppm)	^{19}F NMR (δ) (ppm)
1	**1a**	R^1 = H, R^2 = H	**3a**	58	5.31	−74.78
2	**1b**	R^1 = H, R^2 = Me	**3b**	65	5.29	−74.96
3	**1c**	R^1 = OMe, R^2 = H	**3c**	47	5.28	−75.04

4.3. Catalytic reactions

Next, Pd-complex **3a** was tested as a catalyst in oxidative cross-coupling reactions (Fig. 8) [10]. When **3a** is used to catalyze the cyclization of substrate **1a**, (i.e. the substrate and ligand are of the same source), the reaction is complete within 24 h, whereas with $Pd(OAc)_2$, the reaction progresses to only 54% yield (Table 5, entries 1 and 2). Complex **3a** also catalyzed the oxidative cross-coupling of other *N*-methyl-*N*-phenylbenzamide substrates. Of note, substrate **1c** yields 64% of the desired phenanthridinone in the presence of catalytic $Pd(OAc)_2$, in contrast to yielding 99% with Pd-complex **3a** (Table 5, entries 3 and 4). Pd-complex **3a** also catalyzed the reaction with substrate **1d** faster than $Pd(OAc)_2$ (Table 5, entries 5 and 6). These results suggest that Pd-complex **3a** is a more reactive precatalyst than $Pd(OAc)_2$ and that $Pd(OAc)_2$ appears to require a longer induction period than Pd-complex **3a**. Palladacycles **3b** and **3c** gave similar results in the catalytic reactions; they

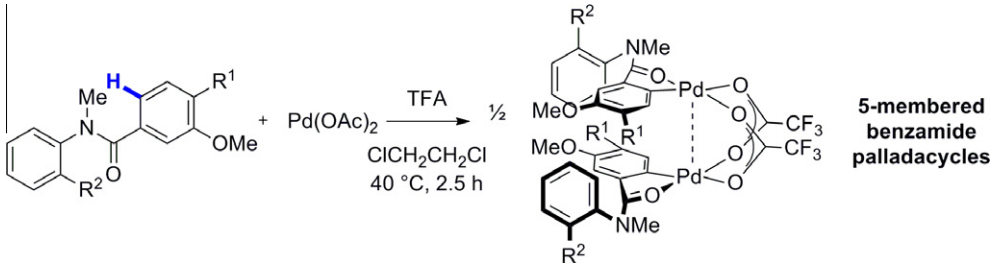

Fig. 6. Synthesis and characterization of the Pd-complexes.

Table 4
Stoichiometric reductive elimination reactions.

Entry	Additive	Time	Yield[a]
1	None	24 h	–
2	TFA, $Na_2S_2O_8$	24 h	21%
3	None	4 days	17%
4	TFA, $Na_2S_2O_8$	4 days	9%

[a] The yield was determined by GC–FID analysis with $C_{14}H_{30}$ as an internal standard.

Table 5
Comparison of Pd(II) catalysts in the oxidative intramolecular cross-coupling reaction.

Entry	R^1, R^2	Substrate	Catalyst	Time (h)	Yield[a] (%)
1	R^1 = H, R^2 = OMe	**1a**	**3a**	24	90
2	R^1 = H, R^2 = OMe	**1a**	$Pd(OAc)_2$	24	54
3	R^1, R^2 = OMe	**1c**	**3a**	24	99
4	R^1, R^2 = OMe	**1c**	$Pd(OAc)_2$	24	64
5	R^1, R^2 = H	**1d**	**3a**	24	60
6	R^1, R^2 = H	**1d**	$Pd(OAc)_2$	24	33

[a] The yield was determined by GC–FID analysis with $C_{14}H_{30}$ as an internal standard.

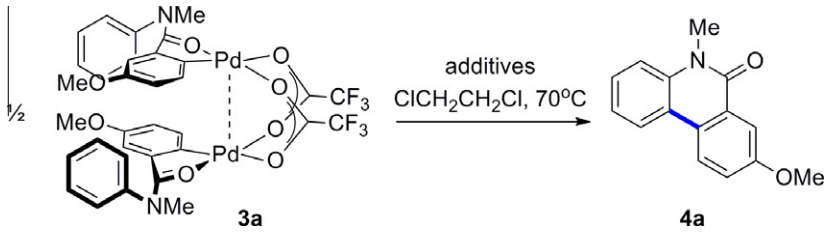

Fig. 7. Stoichiometric reductive elimination reactions.

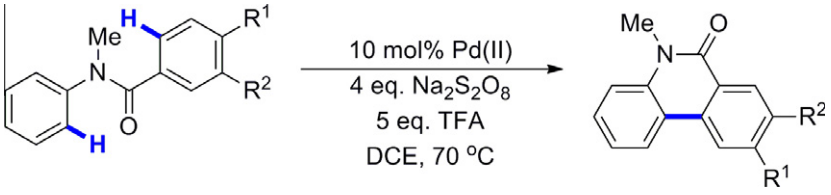

Fig. 8. Comparison of Pd(II) catalysts in the oxidative intramolecular cross-coupling reaction.

catalyze the intramolecular oxidative arylation more efficiently than $Pd(OAc)_2$.

5. Conclusion

In summary, three novel dimeric TFA-bridged palladium(II) complexes have been isolated from an *ortho*-palladation reaction. Single crystal X-ray structures were obtained for Pd-complexes **3a**, **3b** and **3c** and these structures establish a regioselective C–H bond activation to form five-membered palladacycles. Pd-complex **3a** undergoes reductive elimination at 70 °C to give phenanthridinone with low efficiency. Nonetheless, Pd-complex **3a** is an effective precatalyst for oxidative cross-coupling reactions. Further investigation into the mechanism of this transformation is warranted.

Acknowledgments

Funding was provided by the University of Toronto, Canada Foundation for Innovation, Ontario Research Fund, Boehringer Ingelheim Ltd. (Canada), and the Natural Sciences and Engineering Research Council (NSERC) of Canada. V.M.D. is grateful for an Alfred P. Sloan fellowship and N.B. is grateful for the NSERC André Hamer Postgraduate Prize and the Julie Payette Research Scholarship. The authors thank Paul DiCarmine and Professor Dwight Seferos for helpful discussions.

Appendix A. Supplementary material

Supplementary data associated with this article can be found, in the online version, at doi:10.1016/j.ica.2011.01.059.

References

[1] For examples of intramolecular oxidative arylations, see: (a) B. Liegault, D. Lee, M.P. Huestis, D.R. Stuart, K. Fagnou, J. Org. Chem. 73 (2008) 5022;
(b) T. Watanabe, S. Oishi, N. Fujii, H. Ohno, J. Org. Chem. 74 (2009) 4720;
(c) V. Sridharan, M.A. Martin, J.C. Menendez, Eur. J. Org. Chem. (2009) 4614;
(d) H. Hagelin, J.D. Oslob, B. Akermark, Chem.-Eur. J. 5 (1999) 2413;
(e) B.-J. Li, S.-D. Yang, Z.-J. Shi, Synlett (2008) 949;
(f) K. Wang, Y. Hu, Z. Li, M. Wu, Z. Liu, B. Su, A. Yu, Y. Liu, Q. Wang, Synthesis 7 (2010) 1083;
(g) B.-X. Tang, R.-J. Song, C.-Y. Wu, Y. Liu, M.-B. Zhou, W.-T. Wei, G.-B. Deng, D.-L. Yin, J.-H. Li, J. Am. Chem. Soc. 132 (2010) 8900;
(h) M.N. Hopkinson, A. Tessier, A. Salisbury, G.T. Giuffredi, L.E. Combettes, A.D. Gee, V. Gouverneur, Chem. Eur. J. 16 (2010) 4739;
(i) S. Hernandez, I. Moreno, R. SanMartin, G. Gomez, M.T. Herrero, E. Dominguez, J. Org. Chem. 75 (2010) 434;
(j) T.A. Dwight, N.R. Rue, D. Charyk, R. Josselyn, B. DeBoef, Org. Lett. 9 (2007) 3137;
(k) D.G. Pintori, M.F. Greaney, J. Am. Chem. Soc. 133 (2011) 1209.

[2] For selected examples of oxidative cross-coupling involving twofold C–H functionalization, see: (a) D.R. Stuart, K. Fagnou, Science 316 (2007) 1172;
(b) D.R. Stuart, E. Villemure, K. Fagnou, J. Am. Chem. Soc. 129 (2007) 12072;
(c) K.L. Hull, M.S. Sanford, J. Am. Chem. Soc. 129 (2007) 11904;
(d) K.L. Hull, M.S. Sanford, J. Am. Chem. Soc. 131 (2009) 9651;
(e) B.-J. Li, S.-L. Tian, Z. Fang, Z.-J. Shi, Angew. Chem., Int. Ed. 47 (2008) 1115;
(f) G. Brasche, J. Garcia-Fortanet, S.L. Buchwald, Org. Lett. 10 (2008) 2207;
(g) S.H. Cho, S.J. Hwang, S. Chang, J. Am. Chem. Soc. 130 (2008) 9254;
(h) S. Potavathri, A.S. Dumas, T.A. Dwight, G.R. Naumiec, J.M. Hammann, B. DeBoef, Tetrahedron Lett. 49 (2008) 4050;
(i) J.-B. Xia, S.-L. You, Organometallics 26 (2007) 4869;
(j) R. Li, L. Jiang, W. Lu, Organometallics 25 (2006) 5973;
(k) X. Zhao, C.S. Yeung, V.M. Dong, J. Am. Chem. Soc. 132 (2010) 5837;
For reviews on other oxidative couplings, see: (l) J.A. Ashenhurst, Chem. Soc. Rev. 39 (2010) 540;
(m) G.P. McGlacken, L.M. Bateman, Chem. Soc. Rev. 38 (2009) 2447.

[3] C.S. Yeung, X. Zhao, N. Borduas, V.M. Dong, Chem. Sci. 1 (2010) 331.

[4] Z. Otwinowski, W. Minor, Methods in enzymology, in: C.W. Carter, R.M. Sweet (Eds.), Macromolecular Crystallography, Part A, vol. 276, Academic Press, London, 1997, p. 307.

[5] R.H. Blessing, Acta Crystallogr., Sect. A 51 (1995) 33.

[6] G.M. Sheldrick, Acta Crystallogr., Sect. A 64 (2008) 112.

[7] J.E. Bercaw, A.C. Durrell, H.B. Gray, J.C. Green, N. Hazari, J.A. Labinger, J.R. Winkler, Inorg. Chem. 49 (2010) 1801.

[8] For examples of TFA-bridged Pd-dimers, see: (a) F. Aloui, B. Ben Hassine, Tetrahedron Lett. 50 (2009) 4321;
(b) D. Roiban, E. Serrano, T. Soler, I. Grosu, C. Cativiela, E.P. Urriolabeitia, Chem. Commun. 31 (2009) 4681;
(c) C.M. Frech, G. Leitus, D. Milstein, Organometallics 27 (2008) 894;
(d) R.B. Bedford, M. Betham, J.P.H. Charmant, M.F. Haddow, A.G. Orpen, L.T. Pilarsk, Organometallics 26 (2007) 6346;
(e) P.L. Ruddock, D.J. Williams, P.B. Reese, Steroids 69 (2004) 193;
(f) T.A. Stromnova, D.V. Paschenko, L.I. Boganova, M.V. Daineko, S.B. Katser, A.V. Chukarov, L.G. Kuz'mina, J.A.K. Howard, Inorg. Chim. Acta 350 (2003) 283;
(g) I. Schwarz, J. Rust, C.W. Lehmann, M. Braun, J. Organomet. Chem. 605 (2000) 109;
(h) T.A. Stromnova, S.T. Orlova, D.N. Kazyul'kin, I.P. Stolyarov, I.L. Eremenko, Russ. Chem. Bull. 49 (2000) 150;
(i) A. Vitagliano, B. Åkermark, S. Hansson, Organometallics 10 (1991) 2592;
(j) R. Goddard, C. Krüger, R. Mynott, M. Neumann, G. Wilke, J. Organomet. Chem. 454 (1993) C20;
(k) B.M. Trost, P.J. Metzner, J. Am. Chem. Soc. 102 (1980) 3572;
. For trimeric Pd(μ-TFA) structures see:(l) R.E. Podobedov, T.A. Stromnova, Russ. J. Coord. Chem. 34 (2008) 780.

[9] For recent examples of high oxidation Pd-dimers, see: (a) D.C. Powers, T. Ritter, Nat. Chem. 1 (2009) 302;
(b) D.C. Powers, D. Benitez, E. Tkatchouk, W.A. Goddard III, T. Ritter, J. Am. Chem. Soc. 132 (2010) 14092;
(c) D.C. Powers, D.Y. Xiao, M.A.L. Geibel, T. Ritter, J. Am. Chem. Soc. 132 (2010) 14530;
(d) N.R. Deprez, M.S. Sanford, J. Am. Chem. Soc. 131 (2009) 11234;
For a review on high oxidation state palladium catalysis, see: (e) K. Muniz, Angew. Chem., Int. Ed. 48 (2009). 9412.

[10] For recent examples of catalytically active bimetallic Pd(II)-dimers obtained via C–H activation, see: (a) C.S. Yeung, X. Zhao, N. Borduas, V.M. Dong, Chem. Sci. 1 (2010) 331;
(b) X. Zhao, C.S. Yeung, V.M. Dong, J. Am. Chem. Soc. 132 (2010) 5837;
(c) D.C. Powers, M.A.L. Geibel, J.E.M.N. Klein, T. Ritter, J. Am. Chem. Soc. 131 (2009) 17050;
(d) Y.-J. Wu, F. Yang, J.-L. Zhang, X.-L. Cui, J.-F. Gong, M.-P. Song, T.-S. Li, Chin. Sci. Bull. 55 (2010) 2784–2793;
(e) M.S. Subhas, S.S. Racharlawar, B. Sridhar, P.K. Kennady, P.R. Likhar, M.L. Kantam, S.K. Bhargava, Chem. Commun. 8 (2010) 3001;
(f) J. Zhou, X. Li, H. Sun, J. Organomet. Chem. 695 (2010) 297;
(g) A. Del Zotto, F.I. Prat, W. Baratta, E. Zangrando, P. Rigo, Inorg. Chim. Acta 362 (2009) 97;
(h) X. Jia, D. Yang, S. Zhang, J. Cheng, Org. Lett. 11 (2009) 4716;
(i) R. Giri, J.K. Lam, J.-Q. Yu, J. Am. Chem. Soc. 132 (2010) 686;
(j) Y.-H. Zhang, B.-F. Shi, J.-Q. Yu, Angew. Chem., Int. Ed. 48 (2009) 6097;
(k) Y.-H. Zhang, B.-F. Shi, J.-Q. Yu, J. Am. Chem. Soc. 131 (2009) 5072;
For a review on palladacycles and their use in catalysis, see: (l) J. Dupont, C.S. Consorti, J. Spencer, Chem. Rev. 105 (2005) 2527;
(m) T.W. Lyons, M.S. Sanford, Chem. Rev. 110 (2010) 1147 (and references therein);
For a review on Pd(II)-catalyzed C–H activation, see: (n) X. Chen, K.M. Engle, D.-H. Wang, J.-Q. Yu, Angew. Chem., Int. Ed. 48 (2009) 5094.